Inhibitors of ERp44, PDIA1, and AGR2 induce disulfide-mediated oligomerization of Death Receptors 4 and 5 and cancer cell death

[1]Mary E. Law, [2]Elham Yaaghubi, [2]Amanda F. Ghilardi, [1]Bradley J. Davis, [2]Renan B. Ferreira, [3]Jin Koh, [3,4]Sixue Chen, [2]Sadie F. DePeter, [2]Christopher M. Schilson, [5]Chi-Wu Chiang, [6,7]Coy D. Heldermon, [8]Peter Nørgaard, [2,7]Ronald K. Castellano[#], and [1,7]Brian K. Law[#]

Affiliations

[1]Department of Pharmacology & Therapeutics, University of Florida, Gainesville, FL 32610 USA.

[2]Department of Chemistry, University of Florida, Gainesville, FL 32611 USA.

[3]Proteomics and Mass Spectrometry Facility, Interdisciplinary Center for Biotechnology Research, University of Florida, Gainesville, FL 32610 USA.

[4]Department of Biology, Genetics Institute, University of Florida, Gainesville, FL 32610 USA

[5]Institute of Molecular Medicine, College of Medicine and Center for Infectious Disease and Signaling Research, National Cheng Kung University, Tainan, Taiwan.

[6]Department of Medicine, University of Florida, Gainesville, FL 32610 USA.

[7]UF-Health Cancer Center, University of Florida, Gainesville, FL 32610 USA.

[8]Department of Pathology, Copenhagen University Hospital Herlev, DK-2730 Herlev, Denmark.

[#]Co-Contributing Corresponding Authors

Addresses of Corresponding Authors

Brian K. Law

1200 Newell Drive

Room R5-210 Academic Research Building

University of Florida

P.O. Box 100267

Gainesville, FL 32610

Email: bklaw@ufl.edu Phone: (352) 273-9423

Ronald K. Castellano

Department of Chemistry

University of Florida

P.O. Box 117200

Gainesville, FL 32611

Email: castellano@chem.ufl.edu Phone: (352) 392-2752

Conflict of Interest

The Authors have no conflicts of interest to declare.

Running Title: Molecular Targets of DDAs

Abstract

Breast cancer mortality remains unacceptably high, indicating a need for safer and more effective therapeutic agents. Disulfide bond Disrupting Agents (DDAs) were previously identified as a novel class of anticancer compounds that selectively kill cancers that overexpress the Epidermal Growth Factor Receptor (EGFR) or its family member HER2. DDAs kill EGFR+ and HER2+ cancer cells via the parallel downregulation of EGFR, HER2, and HER3 and activation/oligomerization of Death Receptors 4 and 5 (DR4/5). However, the mechanisms by which DDAs mediate these effects are unknown. Affinity purification analyses employing biotinylated-DDAs reveal that the Protein Disulfide Isomerase (PDI) family members AGR2, PDIA1, and ERp44 are DDA target proteins. Further analyses demonstrate that shRNA-mediated knockdown of AGR2 and ERp44, or expression of ERp44 mutants, alter basal and DDA-induced DR5 oligomerization. DDA treatment of breast cancer cells disrupts PDIA1 and ERp44 mixed disulfide bonds with their client proteins. Together, these results reveal DDAs as the first small molecule, active site inhibitors of AGR2 and ERp44, and demonstrate roles for AGR2 and ERp44 in regulating the activity, stability, and localization of DR4 and DR5, and activation of Caspase 8.

Key Words: Apoptosis, Endoplasmic Reticulum Stress, Cancer, Disulfide bond Disrupting Agents, DR5, DR4, EGFR, AGR2, ERp44, PDIA1, ERAP1

67 **Introduction**

68 In spite of significant improvements in early detection, and new molecularly targeted
69 therapeutics, breast cancer remains the second largest cancer killer of women in America after
70 lung cancer, and is the most frequently diagnosed cancer in American women [1]. Much of the
71 lethality of breast cancer derives from our inability to successfully treat patients with metastatic
72 and/or drug-resistant malignancies. New drugs are needed that bypass resistance to currently
73 used regimens by targeting cancer cell-specific vulnerabilities. A class of agents termed
74 Disulfide bond Disrupting Agents (DDAs) was previously identified and shown to kill breast
75 cancer cells in association with downregulation of the HER-family proteins EGFR, HER2, and
76 HER3, and decreased activating phosphorylation of the Akt kinase [2]. Subsequent work
77 showed that DDAs induce endoplasmic reticulum stress (ERS) [3] and alter the pattern of
78 disulfide bonding of EGFR and the TRAIL receptors, Death Receptor 4 (DR4) and Death
79 Receptor 5 (DR5) [4]. DDA-induced cell death is mediated by activation of the Caspase 8-
80 Caspase 3 extrinsic apoptotic cascade.

81 Little is known regarding how the disulfide bonding of HER-family and Death Receptor-
82 family proteins are chaperoned within the endoplasmic reticulum, and how the disulfide
83 bonding patterns of these proteins control their stability, intracellular localization, and
84 downstream signaling. TNF-Related Apoptosis Inducing Ligand (TRAIL) has been considered
85 a promising cancer therapeutic agent due to its selectivity for killing cancer cells, while leaving
86 normal tissues unharmed [5-8]. However, TRAIL analogs and DR4/5 agonistic antibodies have
87 yet to be clinically approved for anticancer therapy. This is due in part to pharmacokinetic
88 issues related to these protein drugs themselves, and in part to the ability of cancer cells to
89 acquire resistance through a variety of mechanisms, including downregulation of DR4 and

90 DR5 (reviewed in [9]). Since DDAs upregulate DR5 and activate DR4 and DR5 in a ligand-
91 independent manner [4, 10], DDAs may overcome the resistance mechanisms that suppress
92 the efficacy of other activators of the TRAIL/Death Receptor pathway. A recent report showed
93 that the extracellular domain of DR5 prevents oligomerization and downstream activation of
94 Caspase 8 in the absence of ligand engagement, and that excision of the DR5 extracellular
95 domain permits full activation of DR5 in a ligand-independent manner [11]. It was previously
96 proposed that DDAs activate DR5 in a ligand-independent manner by permitting inter-
97 molecular disulfide bond formation at the expense of intramolecular disulfide bonding, resulting
98 in DR5 oligomerization and activation [4, 10]. However, the precise mechanisms by which this
99 happens are unknown. Similarly, DDA treatment causes disulfide bond-dependent EGFR
100 oligomerization followed by degradation [2, 4], but how DDAs perturb EGFR disulfide bonding
101 is unknown. The Protein Disulfide Isomerase (PDI) family member AGR2 is essential for EGFR
102 folding and surface localization [12], and likewise facilitates expression of Mucins [13, 14].
103 The PDI family contains 21 members (reviewed in [15]). Canonical PDIs are considered
104 promising targets for anticancer therapeutics [16] and significant attention has focused on the
105 roles of canonical PDIs in mediating disulfide bond formation via their active site thioredoxin-
106 like CXXC motifs. However, other PDI family members are less well studied. The PDIs AGR2
107 and AGR3 contain a non-canonical CXXS active site motif. Based on biochemical PDI
108 mutagenesis studies [17] it is predicted that AGR2/3 will exhibit disulfide isomerase activity, but
109 not oxidase or reductase activity. Consistent with this, AGR2 forms stable mixed disulfide
110 bonds with its client proteins [12, 13]. Another PDI family member, ERp44, also contains an
111 active site CXXS motif, and has multiple functions within the endoplasmic reticulum (ER).
112 ERp44 plays a critical role in the disulfide-mediated oligomerization of Adiponectin [18, 19]

113 and Immunoglobulin M [20, 21]. Additionally, ERp44 anchors client/partner proteins such as
114 ERO1α, Prx4, FGE/SUMF1, and ER Aminopeptidase 1 (ERAP1) [22-25] that do not possess
115 C-terminal -KDEL ER retention sequences to prevent their secretion (reviewed in [26]).
116 HER-family proteins are the only sub-family of receptor tyrosine kinases that contain
117 two cysteine-rich repeats in their extracellular domain [27]. DR4 and DR5 also harbor
118 numerous disulfide bonds in their extracellular domains [28]. Based on these observations, we
119 previously hypothesized that HER-family proteins and DR4/5 may be particularly sensitive to
120 agents that impede native disulfide bond formation. The mechanisms by which DDAs cause
121 downregulation of EGFR, HER2, and HER3, and activate DR4/5 are unknown. Here we show
122 using novel biotinylated DDA derivatives that DDAs covalently modify ERp44, PDIA1, and
123 AGR2 both in vitro and in intact cells, and that DDA treatment of cells disrupts PDIA1 and
124 ERp44 disulfide bonds with their client proteins, and disulfide-mediated AGR2 dimerization.
125 Together, the results indicate that DDAs activate DR4/5 by inhibiting the activity of the PDI
126 family members ERp44, PDIA1, and AGR2. DDAs are the first agents to our knowledge that
127 function in part by modifying the active site Cys residues of ERp44 and AGR2.

128 **Results**

129 *Characterization of novel DDAs with enhanced potency:* Previously described DDAs, including
130 RBF3, DTDO, and tcyDTDO (Fig. 1A), were demonstrated to suppress tumor growth through
131 induction of apoptotic cancer cell death [4, 29]. As shown in our previous studies, modifications
132 of the parent cyclic DDA, DTDO, resulted in a more potent DDA, tcyDTDO, with improved
133 pharmacodynamic and pharmacokinetic properties [4, 10, 29]. With tcyDTDO in hand, we then
134 explored the effect of substitutions on its cyclohexane ring to determine if its potency and drug-
135 like properties could be further improved. Our efforts led to the design and synthesis of novel
136 DDAs including dimethoxy-tcyDTDO (dMtcyDTDO) and difluoro-tcyDTDO (dFtcyDTDO) (Fig.
137 1B). Well appreciated, fluorine's size and high electronegativity lead to strong C–F bonds that
138 resist metabolic degradation making fluorine substitution an effective way to increase drug
139 stability. For instance, replacing hydrogen with fluorine significantly alters the rate and extent of
140 Cytochrome P450 metabolism [30-33]. Both dMtcyDTDO and dFtcyDTDO exhibit
141 approximately two-fold greater potency than tcyDTDO in cell viability assays (Fig. 1C).
142 DMtcyDTDO also exhibited two-fold greater potency than tcyDTDO in DNA and protein
143 synthesis assays (Fig. S1A). DDAs were previously shown to induce apoptotic cell death
144 associated with ERS, disulfide bond-mediated oligomerization of Death Receptors 4 and 5
145 (DR4/5) and EGFR, and upregulation of DR5 [2-4, 29]. Therefore, we examined the effect of
146 the novel DDAs on disulfide bonding of these proteins by immunoblot analysis under non-
147 reducing conditions ([4] and Supplemental Information). When applied to cancer cells at the
148 same concentration, dMtcyDTDO and dFtcyDTDO induced more DR4/5 oligomerization,
149 higher DR5 levels, and greater ERS (Fig. 1D, left panel). Induction of ERS by dFtcyDTDO and
150 dMtcyDTDO, was indicated by GRP78 elevation, and disulfide-mediated oligomerization of

151 DR4 and EGFR, and oligomerization of DR5 was observed at 1.25 μM of each dFtcyDTDO or
152 dMtcyDTDO (Fig. 1D, right panel). Additional immunoblot analyses performed under reducing
153 conditions revealed that dMtcyDTDO is more potent than tcyDTDO in the induction of HER3
154 downregulation, DR5 upregulation, and ERS as indicated by elevated CHOP and XBP1s (Fig.
155 S1B). Time-course and concentration-response analyses of these endpoints showed that
156 dMtcyDTDO induced these responses as early as four hours after treatment (Fig. S1C).
157 Quantitation of dMtcyDTDO effects on the levels and state of oligomerization of DR4
158 and DR5 revealed that dMtcyDTDO increases DR4 oligomerization without affecting overall
159 DR4 levels, while dMtcyDTDO increases the levels of both oligomeric and monomeric forms of
160 DR5 (Fig. 1E). Tumor studies using the HER2+ BT474 xenograft model [2] were performed to
161 examine if dMtcyDTDO and dFtcyDTDO induce rapid breast cancer cell death in mice bearing
162 palpable breast tumors. Tumors from animals treated with the vehicle for four consecutive
163 days did not show evidence of tumor necrosis (Fig. 1F). In contrast, tumors were not observed
164 in mammary fat pads from dFtcyDTDO treated animals. Mammary glands from dMtcyDTDO
165 treated animals exhibited tumors that had undergone coagulation necrosis, consistent with
166 rapid and uniform death of the cancer cells.
167
168 *AGR2 as a DDA binding protein*: To understand how DDAs kill breast tumors, identification of
169 their direct protein targets is essential. The development of molecular probes proved crucial in
170 identifying DDA biological targets and linking them to the observed DDA responses. For this
171 purpose, we used activity-based protein profiling and standard affinity pulldown techniques
172 with biotin as the affinity label.

173 To generate DDA probes, we sought a biologically active cyclic DDA with a functional
174 group that enables installation of a biotin tag. This was achieved by fusing a Boc-protected
175 pyrrolidine ring at the 4,5-positions of the parent DTDO compound to generate (±)-
176 BocPyrDTDO (Fig. 2A), which is biologically active and showed a potency similar to DTDO
177 (Fig. S1D). The synthesis of (±)-BocPyrDTDO was accomplished by cleaving the acetyl groups
178 of dithioacetate (±)-**3** followed by oxidation to furnish the 1,2-dithiane 1,1-dioxide ring (Fig. 2A).
179 Intermediate (±)-**3** can be obtained through a few functional group interconversion steps from
180 diester (±)-**1** which itself could be obtained according to literature procedures. The amino
181 group on the pyrrolidine ring, after Boc group deprotection, enables installation of the linker
182 and biotin tag as described in full detail in the Supplemental Information. Biotinylated DDA
183 analogs, including Biotin-PyrDTDO (BPD) and Biotin-GlyPyrDTDO (BGPD), were generated in
184 this fashion and used as affinity tags to identify DDA bound proteins (Fig. 2A).
185 The protein disulfide isomerase (PDI) family member AGR2 was previously implicated
186 in disulfide bonding of EGFR [12], and DDAs alter EGFR disulfide bonding ([4] and Fig. 1D,
187 right panel). We hypothesized that AGR2 might be a target of DDAs and examined if
188 biotinylated DDAs bind covalently with recombinant AGR2. Biotin-GlyPyrDTDO labeled AGR2
189 in a concentration-dependent manner (Fig. 2B). Under these conditions, Biotin-GlyPyrDTDO
190 labeled monomeric, but not disulfide bonded dimeric AGR2. We further hypothesized that in
191 addition to EGFR, DR4 or DR5 may be AGR2 client proteins. Stable knockdown of AGR2 in
192 breast cancer cells increased disulfide-mediated DR5 oligomerization in the absence of DDA
193 treatment (Fig. 2C). AGR2 forms mixed disulfide bonds to its client proteins with Cys81 in its
194 thioredoxin-like repeat [13], and Cys81 is the only Cys residue present in AGR2. Therefore, we
195 examined if mutating Cys81 to Ser prevented DDA labeling. The C81S AGR2 mutant was not

196 labeled by Biotin-GlyPyrDTDO (Fig. 2D). AGR3 is the PDI paralog most closely related to
197 AGR2 and it was also labeled by Biotin-GlyPyrDTDO. Addition of a molar excess of
198 dMtcyDTDO to the labeling reactions partially prevented Biotin-GlyPyrDTDO binding to AGR2
199 and AGR3 (Fig. 2D), suggesting competition for binding to the same Cys residue(s). A
200 comparison of the ability of dMtcyDTDO and tcyDTDO to block Biotin-GlyPyrDTDO binding to
201 AGR2 indicated that dMtcyDTDO was a more effective competitor, indicating that competition
202 in this binding assay reflects DDA potency (Fig. 2E, S1E, S1F). AGR2 is expressed at low
203 levels in MDA-MB-468 cells, and disulfide-bonded AGR2 complexes with client proteins were
204 not detected in either the presence or absence of dMtcyDTDO treatment (Fig. 2F). Enforced
205 AGR2 expression revealed formation of dimeric AGR2 that was not observed with the C81S
206 AGR2 active site mutant. Treatment of the cells with dMtcyDTDO blocked dimer formation by
207 wild type AGR2, consistent with blockade of C81S by dMtcyDTDO binding.
208
209 *Identification of PDIA1 and ERp44 as DDA target proteins:* A panel of three breast cancer cell
210 lines was treated with Biotin-PyrDTDO to label DDA target proteins in intact cells. In addition to
211 affinity purification of endogenous biotinylated proteins, such as carboxylases, which use biotin
212 as a cofactor, two biotinylated proteins were observed exclusively in the context of cell labeling
213 with Biotin-PyrDTDO in multiple experiments and termed DDA target proteins 1 and 2
214 (DDAT1/2). DDAT1/2 migrated at 60 kDa and 44 kDa, respectively, and were observed in
215 three different breast cancer lines in crude cell extracts and in samples purified using
216 Streptavidin-agarose (Fig. 3A). The Streptavidin-agarose purification was scaled up to
217 generate DDAT1/2 in sufficient amounts for identification by mass spectrometry, and aliquots
218 of this preparation and the corresponding crude extracts were analyzed by blotting with

219 Streptavidin-Alkaline Phosphatase, and by silver staining (Fig. 3B). DDAT1 and DDAT2 from a
220 Coomassie stained gel were excised and analyzed by trypsin digestion followed by mass
221 spectrometry as described in Materials and Methods. DDAT1 and DDAT2 were identified as
222 the PDI-family members PDIA1 and ERp44, respectively (Fig. S2A, S2B). In support of these
223 assignments, ERp44, PDIA1, and AGR2 were isolated from the luminal A T47D and luminal B
224 BT474 breast cancer cell lines treated with Biotin-PyrDTDO using Streptavidin-Agarose (Fig.
225 3C, left panel). In additional Biotin-PyrDTDO pulldown experiments, ERp44 and PDIA1 were
226 detected, but the PDIs ERp57 and ERp5 were not (Fig. 3D). Endogenous proteins are
227 biotinylated via amide linkages. Thus, DDAT1 and DDAT2 were distinguished from
228 endogenous biotinylated proteins by disruption of Biotin-DDA/target protein linkages with the
229 reducing agent 2-Mercaptoethanol (Fig. S2C). Immunoprecipitation with an AGR2 antibody
230 showed that ERp44 and PDIA1 co-purify with AGR2 from cells irrespective of treatment with
231 Biotin-PyrDTDO (Fig. 3C, left panel). ERp44 immunoprecipitates contained PDIA1, but AGR2
232 co-purification was not detected. Biotin-PyrDTDO/Streptavidin-Agarose also affinity purified
233 ERp44 and PDIA1 from the MDA-MB-468 Triple-Negative breast cancer cell line (Fig. 3C, right
234 panel). In vitro binding studies showed that Biotin-PyrDTDO labeled ERp44 and PDIA1, and in
235 both cases, biotinylation was blocked by pre-incubation with a molar excess of dMtcyDTDO
236 (Fig. 3E). If ERp44 and PDIA1 are cellular DDA targets, then DDA treatment may alter the
237 pattern of ERp44 and PDIA1 disulfide bonding with their client proteins. Consistent with this,
238 treatment of breast cancer cells with dMtcyDTDO reduced disulfide bonding of ERp44 and
239 PDIA1 with multiple proteins (Fig. 3F, red arrows) with minimal effect on monomeric levels of
240 ERp44 and PDIA1. PDIA1 is a validated target for anticancer drugs [16]. However, ERp44 has
241 not been investigated extensively as a therapeutic target for cancer, and small molecule

242 ERp44 inhibitors have not been reported. Small molecule active site AGR2 inhibitors have not
243 been reported, but under the conditions used here, AGR2 binding to client proteins was not
244 detected. Therefore we focused most of our efforts on examining the consequences of ERp44
245 inhibition by DDAs.
246
247 *DDAs block the ER retention function of ERp44:* ERp44 carries out two important functions by
248 disulfide bonding with client proteins and cycling between the Golgi and the ER as modeled in
249 Fig. 4A. First, ERp44 retrotranslocates inappropriately oligomerized proteins from the Golgi to
250 ER for additional rounds of disulfide bond formation and shuffling. Second, ERp44 disulfide
251 bonds with select partner proteins to retain them in the ER/Golgi, preventing their secretion. To
252 determine if DDAs block ERp44 retention of partners by binding to the ERp44 active site,
253 MDA-MB-468 cells were treated with dMtcyDTDO for 24 h and the levels of the ERp44 partner
254 ERAP1 were examined. DMtcyDTDO treatment decreased cellular ERAP1 levels (Fig. 4B).
255 Quantitation of dMtcyDTDO effects on ERAP1 levels and dMtcyDTDO binding to its client
256 proteins across multiple experiments showed that dMtcyDTDO decreased ERAP1 levels and
257 ERp44 binding to client proteins in a statistically significant manner (Fig. 4C, D). ERAP1
258 migrates primarily as a monomer even under nonreducing conditions, indicating that ERAP1
259 disulfide bonding with ERp44 is transient. Enforced expression of wild type ERp44 (CXXS)
260 resulted in the formation of a higher molecular mass band recognized by ERAP1 antibodies
261 (Fig. 4E). This band was not observed when the C58S ERp44 active site mutant (SXXS) was
262 expressed, but was observed when the S61C mutant (CXXC) was expressed. The ERAP1-
263 ERp44 disulfide-bonded dimer was not observed when analyses were performed under

264 reducing conditions (not shown) and was decreased if the cells were treated with the DDA
265 dFtcyDTDO for 24h (Fig. 4E).
266 DDA-induced secretion of ERAP1 was examined by treating MDA-MB-468 breast
267 cancer cells or A431 skin cancer cells with dMtcyDTDO for 24 h and examining ERAP1 levels
268 in cell extracts and in the culture medium. ERAP1 was only observed in the medium upon
269 dMtcyDTDO treatment (Fig. 4F, upper panels), and dMtcyDTDO induced ERAP1 secretion in a
270 statistically significant manner (Fig. 4F, lower panels).
271
272 *A role for ERp44 in the control of Death Receptor and EGFR disulfide bonding:* Immunoblot
273 analysis of a panel of breast cancer cell lines revealed that PDIA1 levels were similar among
274 the lines (Fig. 5A). In contrast, ERp44, AGR2, and AGR3 levels varied among the lines, as did
275 the oxidoreductase ERO1, which plays a key role in producing oxidizing equivalents for
276 disulfide bond formation [16, 34-36]. A BT474 breast cancer cell line stably overexpressing
277 ERp44 was generated to examine the effect of elevated ERp44 levels on DR4/5 disulfide
278 bonding and DDA responses. ERp44 overexpression reduced DDA induction of high molecular
279 mass DR4 oligomers, and to a lesser extent high molecular mass DR5 oligomers (Fig. 5B, left
280 panel, red arrows). In both cases, the overall pattern was a shift from high to lower molecular
281 mass disulfide-bonded species. These oligomeric protein forms were not observed when the
282 analyses were performed under reducing conditions (Fig. 5B, right panel). Next, ERp44
283 knockdown MDA-MB-468 cells were generated and the effect on DR4/5 disulfide bonding was
284 examined. Although we were only able to achieve modest ERp44 knockdown in multiple
285 independent experiments, ERp44 knockdown consistently increased high molecular mass
286 oligomers of DR4, DR5, and EGFR in the absence of DDA treatment (Fig. 5C, red arrows;

287 expanded view in Fig. 5D, red asterisks; Fig. S2D). ERp44 knockdown augmented PDIA1
288 oligomerization and increased dMtcyDTDO induction of Caspase 8 cleavage/activation (CC8).
289 Together, the results of the AGR2 and ERp44 knockdown experiments are consistent with
290 roles for AGR2 and ERp44 in facilitating native disulfide bond formation of DR4 and DR5, and
291 for DDAs in blocking these AGR2 and ERp44 functions. The observation that ERp44
292 knockdown increases PDIA1 binding to clients may indicate that PDIA1 partially compensates
293 for decreased ERp44 function.

294 We next examined if mutations within the thioredoxin-like repeat of ERp44 alter DR5
295 levels and disulfide bonding, and other DDA responses. Overexpressed wild type ERp44
296 exhibited a high level of disulfide bond-mediated oligomer formation with client proteins (Fig.
297 6A). Both endogenous and overexpressed ERp44 monomers migrated as a doublet, which
298 may result from differential O-linked glycosylation [37]. The C58S ERp44 mutant (SXXS),
299 which lacks a Cys residue in its thioredoxin-like repeat, showed lower binding to client proteins,
300 although the levels of the monomer were similar to that of the wild type protein. The S61C
301 ERp44 mutant (CXXC) exhibited slightly increased oligomerization compared with wild type
302 ERp44. We previously showed that DDAs alter the electrophoretic mobility of EGFR and CUB
303 Domain-Containing Protein 1 (CDCP1), block the formation of complexes between these two
304 proteins, and alter their tyrosine phosphorylation patterns [38]. Overexpression of both ERp44
305 point mutants was associated with increased oligomerization of EGFR and CDCP1, but did not
306 alter the ratio between the full length (FL) and cleaved (Cl.) forms of CDCP1. Overexpressed
307 ERp44 exhibited disulfide bonding to client proteins and these interactions were partially
308 blocked by dFtcyDTDO treatment (Fig. 6B, e.g., bands marked by asterisks). As observed in
309 Fig. 6A, the C58S mutant showed decreased binding to client proteins. Interestingly, the S61C

310 ERp44 mutant bound client proteins similarly to the wild type protein, but was less sensitive to
311 disruption of binding to its clients by dFtcyDTDO. ERp44 overexpression had little effect on
312 DR4 levels with or without dFtcyDTDO treatment. In contrast, overexpression of either the
313 C58S or S61C ERp44 mutants modestly increased steady-state DR5 expression and
314 potentiated DR5 upregulation by dFtcyDTDO. Overexpression of ERp44 and its mutants
315 increased PDIA1 levels and binding to its client proteins. Consistent with the C58S ERp44
316 mutant inducing the strongest potentiation of DR5 upregulation by dFtcyDTDO, expression of
317 this mutant was also associated with increased expression of the ERS marker GRP78 (Fig.
318 6B). Overall, these observations indicate that ERp44^{C58S}, and to a lesser extent, ERp44^{S61C},
319 interfere with disulfide bond formation of ERp44 clients, resulting in higher baseline ERS and
320 potentiating DDA effects on DR4 and DR5. However, these observations do not explain why
321 cancer cells that overexpress EGFR or HER2 have heightened DDA sensitivity [2, 3]. T47D
322 breast cancer cells express low levels of EGFR, HER2, and HER3 and were previously used
323 as a model system to study the effects of EGFR overexpression on DDA responses [2, 3, 39].
324 Examination of ERp44 and PDIA1 disulfide bonding in control and EGFR overexpressing T47D
325 cells showed that EGFR overexpression resulted in recruitment of ERp44 and PDIA1, and to a
326 lesser extent DR4/5, into disulfide-bonded protein complexes (Fig. 6C). Under these
327 conditions, levels of monomeric ERp44 and PDIA1 are decreased. Oligomeric, disulfide-
328 bonded forms of ERp44 and PDIA1 are expected to be inaccessible for binding to newly
329 produced client proteins, while the monomeric forms of ERp44 and PDIA1 are accessible to
330 facilitate native disulfide bonding of their client proteins. Thus, EGFR may increase DDA
331 sensitivity by reducing the pools of monomeric ERp44 and PDIA1 that DDAs must inhibit in
332 order to block native disulfide bond formation of ERp44 and PDIA1 client proteins.

333 ERp44 mediates quality control of Adiponectin [18] and Immunoglobulin M [21]
334 maturation by shuttling inappropriately disulfide bonded protein forms from the Golgi back into
335 the ER, while permitting secretion of correctly disulfide bonded proteins. We hypothesized that
336 ERp44, PDIA1, or AGR2 disulfide bonding with DR4 or DR5 may sequester DR4 and DR5 in
337 the ER or Golgi, preventing their trafficking to the cell surface. Therefore, we hypothesized that
338 by blocking active site ERp44, PDIA1, and AGR2 Cys residues, DDA treatment may permit
339 DR4 and DR5 trafficking to the cell surface. Cell labeling using membrane impermeable,
340 protein-reactive probes is useful for confirming the presence of receptors at the cell surface.
341 Surface biotinylation studies performed on cells after treatment with dMtcyDTDO showed
342 increased cell surface levels of DR4 and DR5, irrespective of whether labeling was performed
343 with amine- or thiol-reactive cell-impermeable biotinylation probes (Fig. 6D). This increased
344 accumulation of DR4/5 at the cell surface may explain previous findings showing that DDAs
345 synergize with the DR4/5 ligand TRAIL to induce cancer cell apoptosis [4].
346
347 *DDAs potentiate non-covalent binding of DR5 to ERp44:* Data in Fig. 5 and 6 showing that
348 ERp44 knockdown and overexpression of ERp44 mutants alter DR5 levels or oligomerization
349 suggested that DR5 may be an ERp44 client protein. We reasoned that if DR5 is an ERp44
350 client, the two proteins may bind to each other. ERp44 co-immunoprecipitation experiments
351 showed that ERp44 associates with DR5 and to a lesser extent DR4 in MDA-MB-468 cells,
352 and these interactions were potentiated by DDA treatment (Fig. 7A; Fig. S2E). These were
353 non-covalent ERp44/DR5 complexes because although the analyses were performed under
354 non-reducing conditions, each protein migrated as a monomer. ERp44 co-immunoprecipitation
355 studies were next carried out in cells ectopically expressing ERp44 or the C58S or S61C

356 ERp44 mutants. DR5 immunoprecipitated with wild type ERp44 and the S61C ERp44 mutant,
357 but not the C58S ERp44 mutant (Fig. 7B, left panel). DDA treatment increased DR5 and
358 decreased PDIA1 association with ERp44, which may be partly explained by changes in
359 PDIA1 and ERp44 expression levels (Fig. 7B, right panel). Since DDAs increase DR5 levels,
360 which could account for the increased DR5 binding to ERp44, we used the tet-ON system to
361 drive high-level DR4 or DR5 expression. Doxycycline-induced DR4 expression increased DR4
362 binding to ERp44 and binding was further enhanced by DDA treatment (Fig. 7C). Doxycycline-
363 induced DR5 expression caused detectable DR5 binding to ERp44, which was strongly
364 enhanced by DDA treatment. The results in Fig. 7A-C demonstrate that DR5 forms a non-
365 covalent complex with ERp44 and that formation of this complex is strongly enhanced by DDA
366 treatment. To determine if ERp44 in dMtcyDTDO-treated cells associates with the disulfide
367 bond-rich extracellular domain of DR5, ERp44 immunoprecipitation experiments were
368 performed in cells that inducibly express wild type DR5 or the Δ81-178 DR5 deletion construct
369 lacking part of the disulfide-rich region. The results indicate that while wild type DR5 bound
370 ERp44 in the context of dMtcyDTDO treatment, ERp44 binding to DR5[Δ81-178] was barely
371 detectable (Fig. 7D). This result may indicate that DDA binding to the ERp44 active site Cys
372 residue not only inactivates its catalytic function, but increases its association with the
373 disulfide-rich region of DR5. This may, in turn, prevent catalytically active forms of ERp44,
374 PDIA1, or AGR2 from chaperoning native DR5 disulfide bond formation.
375 The results presented thus far indicate that DDAs alter the disulfide bonding status of
376 DR4 and DR5, and that this is associated with inhibition of ERp44 and PDIA1 binding to their
377 client proteins. However, it is unclear if perturbation of DR5 disulfide bonding mimics the
378 effects of DDAs, which include upregulation of DR5 protein levels and increased pro-apoptotic

379 signaling. This issue was addressed by inducibly expressing DR5 mutants in which a Cys
380 residue was mutated to Ser to disrupt one of the seven DR5 disulfide bonds. The C119S
381 mutant was constructed to disrupt the center/fourth disulfide bond, and the C160S mutant was
382 constructed to disrupt the seventh, most C-terminal DR5 disulfide bond. Induction of ectopic
383 wild type DR5 expression with low concentrations of doxycycline (e.g. 100 ng/ml) weakly
384 increased DR5 expression (Fig. 7E). However, dMtcyDTDO/doxycycline co-treatment further
385 increased DR5 expression, demonstrating DR5 stabilization by DDAs. The C119S and C160S
386 DR5 mutants were highly expressed in both the monomeric and oligomeric forms, and this was
387 associated with Caspase 8 cleavage/activation. DMtcyDTDO treatment modestly increased
388 Caspase 8 cleavage, but did not further increase expression of the C119S or C160S DR5
389 mutants. This suggests that disruption of individual DR5 disulfide bonds may be sufficient to
390 promote high-level DR5 protein expression, oligomerization, and pro-apoptotic signaling.
391

392 **Discussion**

393 *Models for DDA mechanisms of action and compound selectivity:* The findings presented here
394 suggest that DDAs bind to the PDI-family proteins ERp44, PDIA1, AGR2, and AGR3 and block
395 their ability to chaperone the disulfide bonding of subsets of client proteins. The resulting
396 alteration of disulfide bonding causes upregulation of DR5, oligomerization of DR4 and DR5,
397 and accumulation of DR4 and DR5 at the cell surface. Oligomerization of DR4 and DR5
398 causes Caspase 8 activation, which in turn activates Caspase 3 to execute apoptosis.
399 Caspase activation plays a key role in downregulating EGFR and HER2, and decreasing Akt
400 phosphorylation because these DDA responses are largely ablated by a pan-Caspase inhibitor
401 [4]. To our knowledge, DDAs are the first small molecule agents that block the active site Cys
402 residues of ERp44 and AGR2/3. Further, DDAs are the first experimental anticancer agents
403 that trigger DR4 and DR5-mediated Caspase 8 activation by inducing disulfide bond-mediated
404 DR4/5 clustering in the absence of their ligand, TRAIL. A recent report showed that the
405 extracellular domain of DR5 acts to prevent its oligomerization in the absence of TRAIL [11].
406 DDAs may overcome this autoinhibition by altering the conformations of the DR4/5
407 extracellular domains or favoring intermolecular disulfide bonding between DR4/5 extracellular
408 domains over intramolecular disulfide bonding. Consistent with these interpretations,
409 mutational disruption of individual DR5 disulfide bonds is sufficient to trigger its upregulation,
410 oligomerization, and downstream activation of Caspase 8 (Fig. 7E).

411 Previous reports showed that overexpression of EGFR amplifies multiple DDA responses,
412 including ERS induction, DR5 upregulation, HER1-3 downregulation, and reduction of Akt
413 phosphorylation [2-4]. Discovery of ERp44 and PDIA1 as DDA target proteins led to the
414 observation that EGFR overexpression reduced the levels of “free”, monomeric ERp44 and

415 PDIA1 accessible for facilitating native disulfide bonding of client proteins. Since DDAs
416 covalently modify monomeric ERp44 and PDIA1 (Fig. 3), these observations explain the
417 molecular basis for the sensitivity of EGFR-overexpressing cells to DDAs. Given the
418 importance of EGFR as a potential oncogenic driver in a number of cancers, including
419 glioblastoma [40, 41] and Triple-Negative Breast Cancer [42-44], DDAs may have utility
420 against these malignancies.

421 Because of the relative structural simplicity of DDA molecules, the mechanisms
422 responsible for their target protein selectivity are of interest. PDIA1 has been investigated as a
423 target for anticancer therapeutics, and PDIA1 inhibitors have established anticancer efficacy in
424 preclinical models [45, 46]. AGR2 contributes to tumor progression by facilitating EGFR
425 disulfide bonding and surface presentation [47]. However, AGR2 may also be secreted and
426 promote tumor angiogenesis [48, 49] and act on cell surface receptors [50]. Monoclonal
427 antibodies designed to block extracellular AGR2 functions are under development [50, 51], but
428 agents that ablate the essential role of AGR2 in the folding of client proteins are not available.

429 The canonical thioredoxin-like catalytic site motif CXXC is featured in PDIA1 and
430 several other PDI enzymes (reviewed in [15]). Interestingly, AGR2, AGR3, and ERp44 share a
431 non-canonical CXXS thioredoxin-like repeat sequence. A report employing both yeast genetics
432 and biochemical enzyme assays showed that the essential function of the PDI enzyme for
433 yeast cell survival is catalysis of disulfide exchange or “scramblase” activity and that this could
434 be carried out by the CXXS mutant of PDI (PDI^{CXXS}) [17]. Enzyme assays showed that PDI^{CXXS}
435 could reactivate inappropriately disulfide bonded RNAse A via its scramblase activity. In
436 contrast, PDI^{CXXS} was unable to catalyze disulfide bond oxidation or reduction like the wild type
437 PDI^{CXXC} enzyme.

438 The C-terminal Cys residue in the CXXC motif of PDIs accelerates substrate release.
439 Consequently, CXXS substrate-trapping mutants of PDIs have been used to isolate mixed
440 disulfide bonded dimers with their client/substrate proteins [52, 53]. That the CXXS motif is
441 associated with slow client protein off-rate is consistent with the established roles of ERp44 in
442 retaining specific client/partner proteins such as ERO1 [22] and ERAP1 [25] in the ER, and in
443 retrotranslocation of inappropriately disulfide bonded Adiponectin [54, 55] and IgM [21, 56]
444 from the Golgi to the ER (see Fig. 4A). Thus, the CXXS motifs of AGR2, AGR3, and ERp44
445 bound to DDAs may exhibit a slow DDA off-rate for the same reason, and explain in part the
446 selectivity of DDAs for these enzymes. Our current working model for DDA binding to AGR2,
447 AGR3, and ERp44 is shown in Fig. 7F, where binding of Biotin-PyrDTDO is initiated by
448 nucleophilic attack of the thiosulfonate group of Biotin-PyrDTDO by the thiolate nucleophile of
449 the Cys residue of the CXXS motif. This results in reversible ring opening. We hypothesize that
450 the rate of ring closure and DDA compound excision is decreased by stabilization of the open
451 form of the DDA by interaction of the sulfinate group with functional groups in or near the PDI
452 active site. The reason for stable DDA binding to PDIAI, but not ERp57 or ERp5 is unclear
453 since each protein contains two canonical CGHC repeats. Further work is required to
454 determine which PDIA1 Cys binds DDAs and to identify structural features in the local
455 environment that stabilize DDA binding.
456 It is clear from the experiments with intact cancer cells that DDAs alter the disulfide
457 bonding of DR4, DR5, and EGFR and change the pattern of disulfide bonding between ERp44
458 and PDIA1 and their client proteins. It is difficult to compare these DDA actions with those of
459 published PDI inhibitors since most of these studies did not examine perturbation of protein
460 disulfide bonding in cancer cells, but rather examined compound activity in the Insulin

461 reduction/aggregation assay. While the Insulin reduction assay is valuable for optimizing the
462 potency of PDI inhibitors, it may not be salient in instances where disulfide isomerase activity,
463 ER retention, or Golgi-ER retrotranslocation are more important than disulfide oxidase or
464 reductase activity.

465 The presence of 21 different PDIs in humans and the diverse phenotypes of the
466 corresponding knockout mice (e.g., [25, 57-59]) suggest that individual PDIs chaperone the
467 disulfide bonding, ER retention, or Golgi-ER retrotranslocation of different subsets of client
468 proteins. For instance, ERp44 is unique in its ability to retain the aminopeptidase ERAP1 in the
469 ER/Golgi and this results in ERAP1 secretion in ERp44-deficient mice or cell lines [25]. A
470 biological consequence of this is that ERp44 deletion is associated with hypotension in mice
471 since secreted ERAP1 destabilizes Angiotensin II, leading to reduced blood pressure. It will be
472 of interest to determine if DDAs exhibit antihypertensive activity.

473 ERAP1 also functions as a “molecular ruler” to process peptides for loading onto MHC I
474 for presentation to T cells [60-62]. ERAP1 inhibitors or ERAP1 knockdown changes the
475 spectrum of the MHC I-associated peptides that constitute the “immunopeptidome.” Since
476 DDAs cause ERAP1 secretion, it will be important to determine if DDAs alter the
477 immunopeptidome, and if so, how this alters anticancer immunity.

478 In summary, the results presented here establish perturbation of disulfide bonding by
479 inhibition of subsets of PDIs as a new strategy for activating DR5 and DR4 in cancer cells
480 independently of their engagement by agonistic antibodies or TRAIL. Further, DDAs
481 upregulate DR5 and increase DR4 and DR5 localization to the cell surface. Consequently,
482 DDAs may overcome many of the problems associated with TRAIL analogs and agonistic
483 antibodies specific for DR4 and DR5. Additional research is needed to elucidate the

484 mechanisms by which disrupting individual DR5 disulfide bonds increases its expression
485 levels, disulfide-mediated oligomerization, and activation of Caspase 8. In future studies, it will
486 be important to determine if C-S point mutants of DR4 mimic the corresponding DR5 mutants
487 and drive pro-apoptotic signaling. It will also be interesting to examine whether activated point
488 mutants of DR4 and DR5 exhibit the same selectivity for killing cancer cells in preference to
489 normal cells as their ligand, TRAIL.

490 **Materials and Methods**

491

492 **In vivo tumor studies and histochemical analysis**

493 Breast tumor formation was initiated in NOD-SCID-gamma (NSG) mice obtained from Jackson
494 Laboratories (Bar Harbor, ME USA) by injecting 1×10^6 cancer cells into the #4 mammary fat
495 pads as described previously [4]. Animals bearing HER2+ BT474 tumors [2] were treated with
496 the vehicle or 20 mg/kg dMtcyDTDO or dFtcyDTDO by intraperitoneal injection for five
497 consecutive days. Tissue samples fixed in 4% paraformaldehyde/Phosphate-Buffered Saline
498 (PBS) and paraffin-embedded were sectioned and stained with hematoxylin and eosin (H&E)
499 by the University of Florida Molecular Pathology Core (https://molecular.pathology.ufl.edu/).

500

501 **Streptavidin-Agarose Pulldowns**

502 Cells were treated with Biotin-PyrDTDO with or without the pan-Caspase inhibitor Q-VD-OPH
503 to prevent apoptosis (MedChemExpress, Monmouth Junction, NJ USA) for 16 h in 10% FBS–
504 DMEM, followed by the addition of 25 mM *N*-ethylmaleimide (NEM) (Thermo Scientific,
505 Rockford, IL USA) for 20 min at 37°C. Cells were subsequently scraped directly into the media,
506 washed twice with ice-cold PBS, and pelleted by centrifugation. Cells were extracted in buffer
507 (20 mM HEPES (pH 7.4), 1 mM EDTA, 1mM EGTA, 5% Glycerol, 1 nM Microcystin, 1 mM
508 Na_3VO_4, and 40 mM $Na_2H_2P_2O_7$) containing 1% Triton X-100. Samples were sonicated,
509 followed by centrifugation for 20 min at 4°C. The supernatant was pre-cleared with Sepharose
510 CL-6B (Amersham Biosciences AP, Uppsala, Sweden) for 2h at 4°C. Pre-cleared samples
511 were then incubated with Streptavidin (SA)-Agarose (Thermo Scientific, Rockford IL USA) and
512 mixed overnight at 4°C. The SA-Agarose was washed three times with extraction buffer

513 containing 0.1% Triton X-100, and eluted by boiling in 2X-SDS Sample Buffer containing 5 mM
514 biotin. Samples were analyzed by immunoblot, silver stain, or probing with Streptavidin-
515 conjugated Alkaline Phosphatase.
516
517 **Disulfide Bond-mediated Oligomerization**
518 To evaluate protein disulfide bond-mediated oligomerization, cells were treated with DDAs for
519 24 h in 10% FBS–DMEM. Cells were subsequently scraped into the media and pelleted by
520 centrifugation. Cell pellets were extracted directly into boiling 2X-SDS-Sample Buffer
521 containing 100 mM NEM and boiled for 10 min. Samples were sonicated, followed by
522 centrifugation for 20 minutes at room temperature, and subsequently analyzed by SDS-
523 PAGE/immunoblot.
524
525 **Surface Biotinylation**
526 Cell surface proteins were labeled by incubating cells with 1.6 mM Sulfo-NHS-SS-Biotin
527 (Thermo Fisher Scientific, Waltham, MA USA) or 1.6 mM Biotin-dPEG$_3$-Maleimide
528 (MilliporeSigma, St. Louis, MO USA) in PBS, pH 8.0 for 30 minutes at 4 °C. The cells were
529 subsequently washed three times with PBS, and proteins were extracted in 1% Triton X-100
530 extraction buffer in the absence of reducing agents. Cell extracts were then mixed with
531 Streptavidin-agarose beads (Thermo Fisher Scientific, Waltham, MA USA) for 2.5 h at 4°C.
532 Following centrifugation, the supernatant containing non-biotinylated proteins (flow-through)
533 was retained and boiled in 2X-SDS-Sample Buffer containing 1% 2-mercaptoethanol.
534 Streptavidin-agarose beads bound to biotinylated proteins were washed four times with 0.1%
535 Triton X-100 extraction buffer, and eluted by boiling in 2X-SDS-Sample Buffer containing 1%

536 2-mercaptoethanol. Samples were then analyzed by immunoblot or blotting with Streptavidin-
537 conjugated Alkaline Phosphatase.
538
539 **His_6-AGR2 TALON Purification**
540 Competent BL21(DE3) cells were transformed with either the AGR2/pET-45b(+) or AGR2
541 C81S/pET-45b(+) vectors. Protein expression was induced by the addition of 50 μM Isopropyl
542 β-D-1-thiogalactopyranoside (Fisher Scientific, Fair Lawn, NJ USA) to bacterial cell cultures for
543 2.5 hours and shaking at 37°C. Bacterial cells were subsequently pelleted and dissolved in
544 Mouse Tonicity Phosphate Buffered Saline (MTPBS) containing 1% Triton X-100 and
545 sonicated for 20 seconds on ice, followed by centrifugation for 10 min at 4°C to pellet cell
546 debris. The supernatant was transferred to a new tube, followed by the addition of TALON
547 Resin (Clontech, Mountain View, CA USA) and mixed for 30 min at 4°C. The TALON Resin
548 was pelleted by centrifugation and washed twice with MTPBS and twice with MTPBS
549 containing 30 mM Imidazole. Protein bound to the TALON Resin was eluted with 400 mM
550 Imidazole and precipitated with 60% saturated ammonium sulfate. The precipitated protein
551 was pelleted by centrifugation, dissolved in MTPBS containing 1 mM DTT and 1 mM EDTA,
552 and subsequently dialyzed against a solution of MTPBS containing 10 μM DTT and 30%
553 Glycerol.
554
555 **DDA-AGR2 Binding Experiments**
556 Purified His_6-AGR2 or His_6-AGR2[C81S], as prepared above, or His_6-AGR2 (PRO-580) or
557 His_6-AGR3 (PRO-242) obtained from ProSpec (New Brunswick NJ USA) were incubated with
558 or without varying concentrations of the unlabeled DDA competitors, tcyDTDO or dMtcyDTDO,

559 and 30 μM Biotin-GlyPyrDTDO or Biotin-PyrDTDO in buffer (20 mM HEPES (pH 7.4), 1 mM
560 EDTA, 1mM EGTA, 5% Glycerol, 1 nM Microcystin, 1 mM Na_3VO_4, and 40 mM $Na_2H_2P_2O_7$)
561 containing 1% Triton-X 100 for 30 min at 37°C. Preliminary studies showed that Biotin-
562 GlyPyrDTDO or Biotin-PyrDTDO exhibited indistinguishable labeling of proteins in intact cells
563 and purified proteins in vitro. Therefore, the two probes were used interchangeably and are
564 referred to collectively as "Biotin-DDA." Reactions were stopped by boiling the samples in 2X-
565 SDS-Sample Buffer containing 100 mM NEM for 10 min. Biotin-DDA labeling of protein was
566 verified by blotting with Streptavidin-Alkaline Phosphatase (Rockland Immunochemicals, Inc.,
567 Limerick, PA USA). ERp44 (PRO-547) and PDIA1 (ENZ-262) were obtained from ProSpec and
568 used in experiments examining the binding of these proteins to Biotin-PyrDTDO.
569
570 **Quantitative Analysis of Immunoblot Results**
571 Immunoblots were scanned, converted to grayscale and inverted using Adobe Photoshop
572 (Berkeley, CA). Bands were quantified using ImageJ (NIH, Bethesda, MD). Expression levels
573 were normalized using Actin as a loading control.
574
575 **Chemical Synthesis of DDAs**
576 Full experimental and characterization details associated with the synthesis of (±)-
577 BocPyrDTDO, Biotin-GlyPyrDTDO, and Biotin-PyrDTDO are provided in the Supplemental
578 Information. Detailed discussion of the syntheses and analytical characterization of
579 dMtcyDTDO and dFtcyDTDO will be published elsewhere.
580
581 **Detailed Methods in Supplemental Information**

582 At least three biological replicates of each of the studies presented were performed. In-depth
583 descriptions of approaches relating to cell culture, preparation of cell extracts, immunoblot
584 analysis, construction of retroviral and lentiviral vectors and their use to generate stable cell
585 lines, DNA and protein synthesis assays, cell viability assays, sample preparation for analysis
586 by tandem mass spectrometry, and statistical methods are presented in Supplemental
587 Information.

588 **Acknowledgements**

589 These studies were supported in part by grants from the Florida Breast Cancer Foundation (BL
590 and RC), the Ocala Royal Dames for Cancer Research (BL), and the Office of the Assistant
591 Secretary of Defense for Health Affairs through the Breast Cancer Research Program under
592 Award Nos. W81XWH-15-1-0199 (BL) and W81XWH-15-1-0200 (RC), and NIH/NCI grant
593 CA252400 (BL). RF is grateful to the University of Florida for a Graduate School Fellowship.
594 EY thanks the Dr. Howard and Brenda Sheridan Fund in Chemistry for a 2020 Howard and
595 Brenda Sheridan Summer Fellowship. AG is grateful to the Tarrant Organic Chemistry Fund
596 for a 2021 Tarrant Summer Graduate Research Fellowship. Mass spectrometric data on DDA
597 protein targets were obtained by the UF Proteomics and Mass Spectrometry Facility at the
598 Interdisciplinary Center for Biotechnology Research. Mass spectrometric data on DDA
599 compound structures and DDA adducts were obtained by the UF Department of Chemistry
600 Mass Spectrometry Research and Education Center supported, in part, by the National
601 Institutes of Health (NIH S10 OD021758-01A1).

602

603 **Conflicts of Interest**

604 None.

605

606 **References**

607 1 DeSantis CE, Ma J, Gaudet MM, Newman LA, Miller KD, Goding Sauer A *et al*. Breast
608 cancer statistics, 2019. *CA Cancer J Clin* 2019; 69: 438-451.
609
610 2 Ferreira RB, Law ME, Jahn SC, Davis BJ, Heldermon CD, Reinhard M *et al*. Novel
611 agents that downregulate EGFR, HER2, and HER3 in parallel. *Oncotarget* 2015; 6:
612 10445-10459.
613
614 3 Ferreira RB, Wang M, Law ME, Davis BJ, Bartley AN, Higgins PJ *et al*. Disulfide bond
615 disrupting agents activate the unfolded protein response in EGFR- and HER2-positive
616 breast tumor cells. *Oncotarget* 2017; 8: 28971-28989.
617
618 4 Wang M, Law ME, Davis BJ, Yaaghubi E, Ghilardi AF, Ferreira RB *et al*. Disulfide bond-
619 disrupting agents activate the tumor necrosis family-related apoptosis-inducing
620 ligand/death receptor 5 pathway. *Cell Death Discovery* 2019; 5: 153.
621
622 5 Wiley SR, Schooley K, Smolak PJ, Din WS, Huang CP, Nicholl JK *et al*. Identification
623 and characterization of a new member of the TNF family that induces apoptosis.
624 *Immunity* 1995; 3: 673-682.
625
626 6 Rieger J, Naumann U, Glaser T, Ashkenazi A, Weller M. APO2 ligand: a novel lethal
627 weapon against malignant glioma? *FEBS Lett* 1998; 427: 124-128.
628
629 7 Zamai L, Ahmad M, Bennett IM, Azzoni L, Alnemri ES, Perussia B. Natural killer (NK)
630 cell-mediated cytotoxicity: differential use of TRAIL and Fas ligand by immature and
631 mature primary human NK cells. *J Exp Med* 1998; 188: 2375-2380.
632
633 8 Ashkenazi A, Pai RC, Fong S, Leung S, Lawrence DA, Marsters SA *et al*. Safety and
634 antitumor activity of recombinant soluble Apo2 ligand. *J Clin Invest* 1999; 104: 155-162.
635
636 9 Thapa B, Kc R, Uludag H. TRAIL therapy and prospective developments for cancer
637 treatment. *J Control Release* 2020; 326: 335-349.
638
639 10 Wang M, Law ME, Davis BJ, Yaaghubi E, Ghilardi AF, Ferreira RB *et al*. Mechanistic
640 Elucidation of the Antitumor Properties of a Novel Death Receptor 5 Activator. *bioRxiv*
641 2019: 700906.
642
643 11 Pan L, Fu TM, Zhao W, Zhao L, Chen W, Qiu C *et al*. Higher-Order Clustering of the
644 Transmembrane Anchor of DR5 Drives Signaling. *Cell* 2019; 176: 1477-1489 e1414.
645
646 12 Dong A, Wodziak D, Lowe AW. Epidermal growth factor receptor (EGFR) signaling
647 requires a specific endoplasmic reticulum thioredoxin for the post-translational control of
648 receptor presentation to the cell surface. *J Biol Chem* 2015; 290: 8016-8027.
649

650 13 Park SW, Zhen G, Verhaeghe C, Nakagami Y, Nguyenvu LT, Barczak AJ *et al*. The
651 protein disulfide isomerase AGR2 is essential for production of intestinal mucus. *Proc*
652 *Natl Acad Sci U S A* 2009; 106: 6950-6955.
653
654 14 Schroeder BW, Verhaeghe C, Park SW, Nguyenvu LT, Huang X, Zhen G *et al*. AGR2 is
655 induced in asthma and promotes allergen-induced mucin overproduction. *Am J Respir*
656 *Cell Mol Biol* 2012; 47: 178-185.
657
658 15 Galligan JJ, Petersen DR. The human protein disulfide isomerase gene family. *Hum*
659 *Genomics* 2012; 6: 6.
660
661 16 Shergalis AG, Hu S, Bankhead A, 3rd, Neamati N. Role of the ERO1-PDI interaction in
662 oxidative protein folding and disease. *Pharmacol Ther* 2020; 210: 107525.
663
664 17 Laboissiere MC, Sturley SL, Raines RT. The essential function of protein-disulfide
665 isomerase is to unscramble non-native disulfide bonds. *J Biol Chem* 1995; 270: 28006-
666 28009.
667
668 18 Hampe L, Radjainia M, Xu C, Harris PW, Bashiri G, Goldstone DC *et al*. Regulation and
669 Quality Control of Adiponectin Assembly by Endoplasmic Reticulum Chaperone ERp44.
670 *J Biol Chem* 2015; 290: 18111-18123.
671
672 19 Long Q, Lei T, Feng B, Yin C, Jin D, Wu Y *et al*. Peroxisome proliferator-activated
673 receptor-gamma increases adiponectin secretion via transcriptional repression of
674 endoplasmic reticulum chaperone protein ERp44. *Endocrinology* 2010; 151: 3195-3203.
675
676 20 Cortini M, Sitia R. From antibodies to adiponectin: role of ERp44 in sizing and timing
677 protein secretion. *Diabetes Obes Metab* 2010; 12 Suppl 2: 39-47.
678
679 21 Cortini M, Sitia R. ERp44 and ERGIC-53 synergize in coupling efficiency and fidelity of
680 IgM polymerization and secretion. *Traffic* 2010; 11: 651-659.
681
682 22 Otsu M, Bertoli G, Fagioli C, Guerini-Rocco E, Nerini-Molteni S, Ruffato E *et al*.
683 Dynamic retention of Ero1alpha and Ero1beta in the endoplasmic reticulum by
684 interactions with PDI and ERp44. *Antioxid Redox Signal* 2006; 8: 274-282.
685
686 23 Yang K, Li DF, Wang X, Liang J, Sitia R, Wang CC *et al*. Crystal Structure of the
687 ERp44-Peroxiredoxin 4 Complex Reveals the Molecular Mechanisms of Thiol-Mediated
688 Protein Retention. *Structure* 2016; 24: 1755-1765.
689
690 24 Fraldi A, Zito E, Annunziata F, Lombardi A, Cozzolino M, Monti M *et al*. Multistep,
691 sequential control of the trafficking and function of the multiple sulfatase deficiency gene
692 product, SUMF1 by PDI, ERGIC-53 and ERp44. *Hum Mol Genet* 2008; 17: 2610-2621.
693
694 25 Hisatsune C, Ebisui E, Usui M, Ogawa N, Suzuki A, Mataga N *et al*. ERp44 Exerts
695 Redox-Dependent Control of Blood Pressure at the ER. *Mol Cell* 2015; 58: 1015-1027.

696
697 26 Tempio T, Anelli T. The pivotal role of ERp44 in patrolling protein secretion. *J Cell Sci*
698 2020; 133.
699
700 27 Lemmon MA, Schlessinger J. Cell signaling by receptor tyrosine kinases. *Cell* 2010;
701 141: 1117-1134.
702
703 28 Cha SS, Sung BJ, Kim YA, Song YL, Kim HJ, Kim S *et al*. Crystal structure of TRAIL-
704 DR5 complex identifies a critical role of the unique frame insertion in conferring
705 recognition specificity. *J Biol Chem* 2000; 275: 31171-31177.
706
707 29 Wang MX, Ferreira RB, Law ME, Davis BJ, Yaaghubi E, Ghilardi AF *et al*. A novel
708 proteotoxic combination therapy for EGFR+ and HER2+cancers. *Oncogene* 2019; 38:
709 4264-4282.
710
711 30 Bondi A. Van Der Waals Volumes + Radii. *Journal of Physical Chemistry* 1964; 68: 441-
712 +.
713
714 31 Gillis EP, Eastman KJ, Hill MD, Donnelly DJ, Meanwell NA. Applications of Fluorine in
715 Medicinal Chemistry. *Journal of Medicinal Chemistry* 2015; 58: 8315-8359.
716
717 32 Wang J, Sanchez-Rosello M, Acena JL, del Pozo C, Sorochinsky AE, Fustero S *et al*.
718 Fluorine in Pharmaceutical Industry: Fluorine-Containing Drugs Introduced to the
719 Market in the Last Decade (2001-2011). *Chemical Reviews* 2014; 114: 2432-2506.
720
721 33 Park BK, Kitteringham NR, O'Neill PM. Metabolism of fluorine-containing drugs. *Annual*
722 *Review of Pharmacology and Toxicology* 2001; 41: 443-470.
723
724 34 Frand AR, Kaiser CA. The ERO1 gene of yeast is required for oxidation of protein
725 dithiols in the endoplasmic reticulum. *Mol Cell* 1998; 1: 161-170.
726
727 35 Pollard MG, Travers KJ, Weissman JS. Ero1p: a novel and ubiquitous protein with an
728 essential role in oxidative protein folding in the endoplasmic reticulum. *Mol Cell* 1998; 1:
729 171-182.
730
731 36 Bertoli G, Simmen T, Anelli T, Molteni SN, Fesce R, Sitia R. Two conserved cysteine
732 triads in human Ero1alpha cooperate for efficient disulfide bond formation in the
733 endoplasmic reticulum. *J Biol Chem* 2004; 279: 30047-30052.
734
735 37 Sannino S, Anelli T, Cortini M, Masui S, Degano M, Fagioli C *et al*. Progressive quality
736 control of secretory proteins in the early secretory compartment by ERp44. *J Cell Sci*
737 2014; 127: 4260-4269.
738
739 38 Law ME, Ferreira RB, Davis BJ, Higgins PJ, Kim JS, Castellano RK *et al*. CUB domain-
740 containing protein 1 and the epidermal growth factor receptor cooperate to induce cell
741 detachment. *Breast Cancer Res* 2016; 18: 80.

742
743 39 Wang M, Law ME, Davis BJ, Yaaghubi E, Ghilardi AF, Ferreira RB *et al*. Disulfide bond-
744 disrupting agents activate the tumor necrosis family-related apoptosis-inducing
745 ligand/death receptor 5 pathway. *Cell Death Discov* 2019; 5: 153.
746
747 40 Stockhausen MT, Broholm H, Villingshoj M, Kirchhoff M, Gerdes T, Kristoffersen K *et al*.
748 Maintenance of EGFR and EGFRvIII expressions in an in vivo and in vitro model of
749 human glioblastoma multiforme. *Exp Cell Res* 2011; 317: 1513-1526.
750
751 41 Cho J, Pastorino S, Zeng Q, Xu X, Johnson W, Vandenberg S *et al*. Glioblastoma-
752 derived epidermal growth factor receptor carboxyl-terminal deletion mutants are
753 transforming and are sensitive to EGFR-directed therapies. *Cancer Res* 2011; 71: 7587-
754 7596.
755
756 42 Liu D, He J, Yuan Z, Wang S, Peng R, Shi Y *et al*. EGFR expression correlates with
757 decreased disease-free survival in triple-negative breast cancer: a retrospective
758 analysis based on a tissue microarray. *Med Oncol* 2012; 29: 401-405.
759
760 43 de Ruijter TC, Veeck J, de Hoon JP, van Engeland M, Tjan-Heijnen VC. Characteristics
761 of triple-negative breast cancer. *J Cancer Res Clin Oncol* 2011; 137: 183-192.
762
763 44 Toyama T, Yamashita H, Kondo N, Okuda K, Takahashi S, Sasaki H *et al*. Frequently
764 increased epidermal growth factor receptor (EGFR) copy numbers and decreased
765 BRCA1 mRNA expression in Japanese triple-negative breast cancers. *BMC Cancer*
766 2008; 8: 309.
767
768 45 Stojak M, Milczarek M, Kurpinska A, Suraj-Prazmowska J, Kaczara P, Wojnar-Lason K
769 *et al*. Protein Disulphide Isomerase A1 Is Involved in the Regulation of Breast Cancer
770 Cell Adhesion and Transmigration via Lung Microvascular Endothelial Cells. *Cancers*
771 *(Basel)* 2020; 12.
772
773 46 Xu S, Liu Y, Yang K, Wang H, Shergalis A, Kyani A *et al*. Inhibition of protein disulfide
774 isomerase in glioblastoma causes marked downregulation of DNA repair and DNA
775 damage response genes. *Theranostics* 2019; 9: 2282-2298.
776
777 47 Gupta A, Dong A, Lowe AW. AGR2 gene function requires a unique endoplasmic
778 reticulum localization motif. *J Biol Chem* 2012; 287: 4773-4782.
779
780 48 Guo H, Zhu Q, Yu X, Merugu SB, Mangukiya HB, Smith N *et al*. Tumor-secreted
781 anterior gradient-2 binds to VEGF and FGF2 and enhances their activities by promoting
782 their homodimerization. *Oncogene* 2017; 36: 5098-5109.
783
784 49 Jia M, Guo Y, Zhu D, Zhang N, Li L, Jiang J *et al*. Pro-metastatic activity of AGR2
785 interrupts angiogenesis target bevacizumab efficiency via direct interaction with VEGFA
786 and activation of NF-kappaB pathway. *Biochim Biophys Acta Mol Basis Dis* 2018; 1864:
787 1622-1633.

50 Arumugam T, Deng D, Bover L, Wang H, Logsdon CD, Ramachandran V. New Blocking Antibodies against Novel AGR2-C4.4A Pathway Reduce Growth and Metastasis of Pancreatic Tumors and Increase Survival in Mice. *Mol Cancer Ther* 2015; 14: 941-951.

51 Liu AY, Kanan AD, Radon TP, Shah S, Weeks ME, Foster JM *et al*. AGR2, a unique tumor-associated antigen, is a promising candidate for antibody targeting. *Oncotarget* 2019; 10: 4276-4289.

52 Eriksson O, Stopa J, Furie B. Identification of PDI Substrates by Mechanism-Based Kinetic Trapping. *Methods Mol Biol* 2019; 1967: 165-182.

53 Stopa JD, Baker KM, Grover SP, Flaumenhaft R, Furie B. Kinetic-based trapping by intervening sequence variants of the active sites of protein-disulfide isomerase identifies platelet protein substrates. *J Biol Chem* 2017; 292: 9063-9074.

54 Wang ZV, Schraw TD, Kim JY, Khan T, Rajala MW, Follenzi A *et al*. Secretion of the adipocyte-specific secretory protein adiponectin critically depends on thiol-mediated protein retention. *Mol Cell Biol* 2007; 27: 3716-3731.

55 Wolf G. New insights into thiol-mediated regulation of adiponectin secretion. *Nutr Rev* 2008; 66: 642-645.

56 Anelli T, Ceppi S, Bergamelli L, Cortini M, Masciarelli S, Valetti C *et al*. Sequential steps and checkpoints in the early exocytic compartment during secretory IgM biogenesis. *EMBO J* 2007; 26: 4177-4188.

57 Jang I, Pottekat A, Poothong J, Yong J, Lagunas-Acosta J, Charbono A *et al*. PDIA1/P4HB is required for efficient proinsulin maturation and ss cell health in response to diet induced obesity. *Elife* 2019; 8.

58 Torres M, Medinas DB, Matamala JM, Woehlbier U, Cornejo VH, Solda T *et al*. The Protein-disulfide Isomerase ERp57 Regulates the Steady-state Levels of the Prion Protein. *J Biol Chem* 2015; 290: 23631-23645.

59 Nyirimigabo E, Jin M, Yang Z, Wang J, Zhai K, Mao Y *et al*. The role of ERp44 in glucose and lipid metabolism. *Arch Biochem Biophys* 2019; 671: 175-184.

60 Sui L, Gandhi A, Guo HC. Crystal structure of a polypeptide's C-terminus in complex with the regulatory domain of ER aminopeptidase 1. *Mol Immunol* 2016; 80: 41-49.

61 Chang SC, Momburg F, Bhutani N, Goldberg AL. The ER aminopeptidase, ERAP1, trims precursors to lengths of MHC class I peptides by a "molecular ruler" mechanism. *Proc Natl Acad Sci U S A* 2005; 102: 17107-17112.

833 62 Koumantou D, Barnea E, Martin-Esteban A, Maben Z, Papakyriakou A, Mpakali A *et al*.
834 Editing the immunopeptidome of melanoma cells using a potent inhibitor of endoplasmic
835 reticulum aminopeptidase 1 (ERAP1). *Cancer Immunol Immunother* 2019; 68: 1245-
836 1261.
837
838

839

840 **Figure Legends**

841 **Figure 1** – Characterization of new, more potent DDAs that induce rapid tumor regression.

842 A. Representative first and second generation DDAs (RBF3, DTDO, and tcyDTDO) and

843 illustration of interconversion between the linear and cyclic forms of the DDA pharmacophore.

844

845 B. Structures of new tcyDTDO derivatives dMtcyDTDO and dFtcyDTDO.

846

847 C. MDA-MB-468 cells were treated for 24 h with the indicated concentrations of DDAs and cell

848 viability (MTT) assays were performed. Three biological replicates were performed with similar

849 results.

850

851 D. MDA-MB-468 cells were treated for 24 h as indicated and subjected to immunoblot analysis

852 after non-reducing SDS-PAGE. O and M represent disulfide bonded oligomeric and

853 monomeric protein forms, respectively.

854

855 E. Levels and degree of oligomerization of DR4 (left panel) and DR5 (right panel) were

856 determined by densitometry analysis of bands across multiple experiments and subjected to

857 statistical analysis. Values plotted represent averages and error bars represent S.E. P-values

858 for pairwise comparisons were determined using Student's t-test. (N=4 for each treatment

859 group with similar within-group results).

860

861 F. Mice bearing BT474 cell xenograft tumors were treated once daily for five days with vehicle,

862 20 mg/kg dFtcyDTDO, or 20 mg/kg dMtcyDTDO. Two hours after the final treatment,

863 mammary fat pads/tumors were excised and tumor sections were stained with H&E. T denotes
864 tumor tissue, FP indicates mammary fat pads, and CN represents coagulation necrosis.
865
866 **Figure 2** - AGR2 and AGR3 are DDA target proteins.
867 A. Abbreviated synthetic approach and chemical structures of the biotinylated DDA analogs
868 Biotin-PyrDTDO and Biotin-GlyPyrDTDO.
869
870 B. Purified, recombinant AGR2 was reacted with Biotin-GlyPyrDTDO for 1 h at 37°C, resolved
871 by non-reducing SDS-PAGE, transferred to membranes, and probed with Streptavidin-Alkaline
872 Phosphatase, and by anti-AGR2 immunoblot.
873
874 C. Vector control or AGR2 knockdown MDA-MB-468 cells were treated for 24 h as indicated
875 and analyzed by non-reducing (left panels) or reducing (right panels) immunoblot (CC8,
876 Cleaved Caspase 8). Red arrow indicates oligomerized forms of DR5 that are present at
877 higher levels in the AGR2 knockdown cells. O and M represent disulfide bonded oligomeric
878 and monomeric protein forms, respectively.
879
880 D. Biotin-GlyPyrDTDO binding assays performed as in Fig. 2B, employing the C81S AGR2
881 mutant and AGR3 in addition to AGR2. In the indicated samples, the proteins were pre-
882 incubated with 600 μM dMtcyDTDO to determine if this prevented subsequent Biotin-
883 GlyPyrDTDO binding.
884

885 E. AGR2 binding assay performed as in Fig. 2B to examine the relative abilities of pre-
886 incubation of AGR2 with dMtcyDTDO or tcyDTDO to block subsequent binding of Biotin-
887 GlyPyrDTDO.
888
889 F. The indicated MDA-MB-468 stable cell lines were treated for 24 h with 5 μM dMtcyDTDO
890 and subjected to analysis by non-reducing SDS-PAGE/immunoblot. O, D, and M represent the
891 Oligomeric, Dimeric, and Monomeric forms of AGR2 detected. P43/p41 and p18 denote
892 different Caspase 8 cleavage products.
893
894 **Figure 3** - ERp44 and PDIA1 are additional DDA targets.
895 A. Breast cancer cell lines were treated for 16 h with vehicle, 100 μM Biotin-PyrDTDO, or 100
896 μM Biotin-PyrDTDO + 10 μM Q-VD-OPH for 16 h. Biotinylated proteins were isolated using
897 Streptavidin-coated beads and the crude extracts and Streptavidin pulldowns were analyzed
898 by blotting with Streptavidin-Alkaline Phosphatase. Red arrows indicate bands, designated
899 DDAT1 and DDAT2, present exclusively after Biotin-PyrDTDO treatment.
900
901 B. Biotin-PyrDTDO/Streptavidin pulldowns were performed in BT474 and MDA-MB-468 cells.
902 Purified material was analyzed by Streptavidin-Alkaline Phosphatase detection and silver stain.
903
904 C, left panel. The indicated breast cancer lines were treated with vehicle or 100 μM Biotin-
905 PyrDTDO for 16 h and extracts were subjected to Streptavidin-agarose pulldowns, or anti-
906 AGR2 or anti-ERp44 immunoprecipitations. The purified material was analyzed by immunoblot
907 with the indicated antibodies. C, right panel. BT474 and MDA-MB-468 breast cancer lines were

908 treated with vehicle or 100 μM Biotin-PyrDTDO for 16 h and extracts were subjected to
909 Streptavidin-agarose pulldowns. The affinity-purified samples were analyzed by immunoblot.
910
911 D. MDA-MB-468 cells were treated for 24 h with Biotin-PyrDTDO. Cell extracts were subjected
912 to Streptavidin-agarose pulldowns and the beads were washed and eluted by incubation with 1
913 M 2-mercaptoethanol (Elution 1) followed by elution with SDS-sample buffer containing 5 mM
914 biotin (Elution 2). The eluents and the flow-throughs were analyzed by immunoblot (left panel)
915 and probed with Streptavidin-conjugated with Alkaline Phosphatase (right panel).
916
917 E. Binding assays employing recombinant, purified ERp44 and PDIA1. Proteins were labeled
918 with Biotin-PyrDTDO after pretreatment with vehicle or dMtcyDTDO. Reactions were analyzed
919 by non-reducing SDS-PAGE followed by detection with Streptavidin-Alkaline Phosphatase.
920
921 F. MDA-MB-468 cells were treated or 24 h with vehicle (control) or 5 μM dMtcyDTDO. Cell
922 extracts were resolved by non-reducing SDS-PAGE and analyzed by immunoblot with the
923 indicated antibodies. O and M represent disulfide bonded oligomeric and monomeric protein
924 forms, respectively (CC8, Cleaved Caspase 8). Red arrows denote bands stained with ERp44
925 or PDIA1 antibodies that change in intensity with dMtcyDTDO treatment.
926
927 **Figure 4** – DDAs block ER retention of ERAP1 by ERp44
928 A. Model for the role of ERp44 in retrotranslocation of client proteins from the Golgi to the ER
929 and retention of partner proteins within the ER.
930

931 B. Immunoblot analysis of the levels of ERAP1 and MHC I in MDA-MB-468 cells after
932 treatment with dMtcyDTDO for 24 h.
933
934 C. Quantitative analysis of cellular ERAP1 levels in control and dMtyDTDO treated MDA-MB-
935 468 cells across multiple experiments (N=4).
936
937 D. Quantitative analysis of cellular ERp44 binding to client proteins in control and dMtyDTDO
938 treated MDA-MB-468 cells across multiple experiments (N=4).
939
940 E. The indicated stable MDA-MB-468 cell lines were treated for 24 h with dFtcyDTDO and
941 subjected to non-reducing SDS-PAGE followed by immunoblot. O and M represent Oligomeric
942 and Monomeric protein isoforms.
943
944 F. MDA-MB-468 (left panels) or A431 cells (right panels) were treated for 24 h with 5 μM
945 dMtcyDTDO and cell extracts and conditioned culture media were subjected to immunoblot
946 analysis as indicated (upper panels). ERAP1 levels in the cell extracts and culture medium
947 were subjected to statistical analysis (lower panels, N=3).
948
949
950 **Figure 5** - Evidence that disulfide bonding of DR4 and DR5 are regulated by ERp44.
951 A. Immunoblot analysis of the expression levels of EGFR, ERO1-α, AGR2, AGR3, PDIA1, and
952 ERp44 across a panel of breast cancer cell lines. Actin serves as a loading control.
953

954 B. BT474 cells stably expressing ERp44 or transduced with the vector control were treated for
955 24 h with vehicle, 2.5 μM, or 5 μM dMtcyDTDO. Cell extracts were resolved by SDS-PAGE
956 under non-reducing (left panel) or reducing (right panel) conditions and analyzed by
957 immunoblot. O and M are disulfide bonded oligomeric and monomeric protein forms,
958 respectively.
959
960 C. Vector control or ERp44 knockdown MDA-MB-468 cell lines were treated for 24 h with
961 vehicle, 2.5 μM, or 5 μM dMtcyDTDO. Cell extracts were resolved by non-reducing SDS-PAGE
962 and analyzed by immunoblot (CC8, Cleaved Caspase 8). O and M are disulfide bonded
963 oligomeric and monomeric protein bands, respectively.
964
965 D. Expanded portions of the blots from panel C showing high molecular mass bands at the
966 stacking gel/resolving gel interface (SGI). Asterisks denote bands at the SGI that are more
967 prominent in the ERp44 knockdown cells.
968
969 **Figure 6** – Expression of ERp44 thioredoxin-like repeat mutants alters DDA responses.
970 A. Non-reducing immunoblot analysis of vector control MDA-MB-468 cells, or cells
971 overexpressing wild type ERp44, ERp44[C58S], or ERp44[S61C]. O and M are disulfide
972 bonded oligomeric and monomeric protein bands, respectively. M (FL) and M (Cl.) represent
973 the monomeric full-length and cleaved forms of CDCP1, respectively.
974

975 B. Non-reducing immunoblot analysis of the indicated cell lines treated with vehicle or 7.5 μM
976 dFtcyDTDO for 24 h. O and M are disulfide bonded oligomeric and monomeric protein bands,
977 respectively.
978
979 C. Extracts from vector control or EGFR overexpressing T47D cells were analyzed by non-
980 reducing SDS-PAGE followed by immunoblot. O and M are disulfide bonded oligomeric and
981 monomeric protein bands, respectively.
982
983 D. MDA-MB-468 cells were treated for 24 h with vehicle or 2.5 μM dMtcyDTDO. The cells were
984 then subjected to cell surface protein labeling using membrane-impermeable amine- or thiol-
985 reactive biotinylation probes as described in Supplemental Information. Surface proteins were
986 collected using Streptavidin-coated beads and analyzed along with the flow-though (internal,
987 non-biotinylated proteins) by immunoblot.
988
989 **Figure 7** – Scission of DR5 disulfide bonds triggers high-level DR5 expression,
990 oligomerization, and Caspase 8 activation.
991 A. MDA-MB-468 cells were treated for 24 h with 10 μM dMtcyDTDO or vehicle and cell
992 extracts were immunoprecipitated with ERp44 antibody and analyzed by immunoblot under
993 non-reducing conditions.
994
995 B. MDA-MB-468 cells ectopically expressing wild type ERp44 or the C58S or S61C mutants of
996 ERp44 were treated for 24 h with 10 μM dMtcyDTDO or vehicle. Left panels, cell extracts were

997 immunoprecipitated with ERp44 antibody and analyzed by immunoblot. Right panels, crude
998 extracts were analyzed for protein expression levels by immunoblot.
999
1000 C. MDA-MB-468 cells expressing doxycycline-inducible DR4 and DR5 were treated with 1
1001 μg/ml doxycycline, 10 μM dMtcyDTDO, or doxycycline + dMtcyDTDO for 24 h followed by
1002 immunoprecipitation of ERp44 and immunoblot analysis of the immunoprecipitates and crude
1003 lysates.
1004
1005 D. The indicated MDA-MB-468 cell lines stably expressing wild type DR5 or the Δ81-178
1006 mutant lacking part of the disulfide-rich extracellular domain were treated for 24 h as indicated
1007 and subjected to immunoprecipitation with ERp44 antibodies. The immunoprecipitates and
1008 crude cell lysates were analyzed by non-reducing SDS-PAGE/immunoblot. O and M represent
1009 disulfide bonded oligomeric and monomeric protein forms.
1010
1011 E. The indicated stable MDA-MB-468 cell lines were treated for 24 h with 5 μM dMtcyDTDO
1012 and/or 100 ng/ml doxycycline as indicated and subjected to immunoblot analysis after
1013 resolving proteins by non-reducing SDS-PAGE. O and M represent disulfide bonded
1014 oligomeric and monomeric protein forms.
1015
1016 F. Model for how the biotin-labelled DDA biotin-PyrDTDO reacts in a reversible covalent
1017 fashion with the PDI active site thiolate. Covalent DDA binding is associated with ring-opening
1018 and exposure of a nucleophilic sulfinate group; it is hypothesized that favorable interaction of
1019 the DDA sulfinate group by the PDI decreases the rate of DDA self-excision.

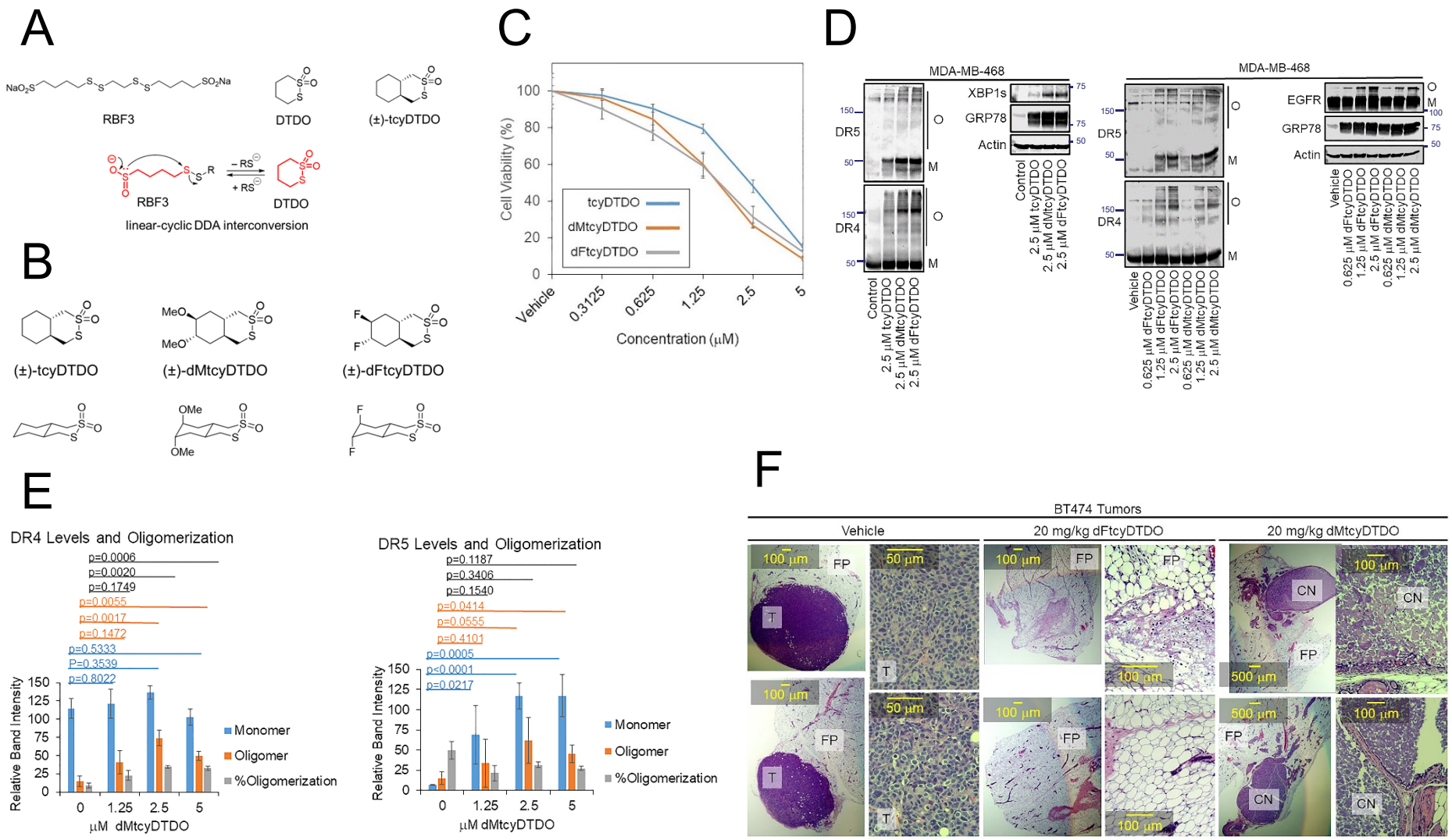

Fig. 1, Law et al.

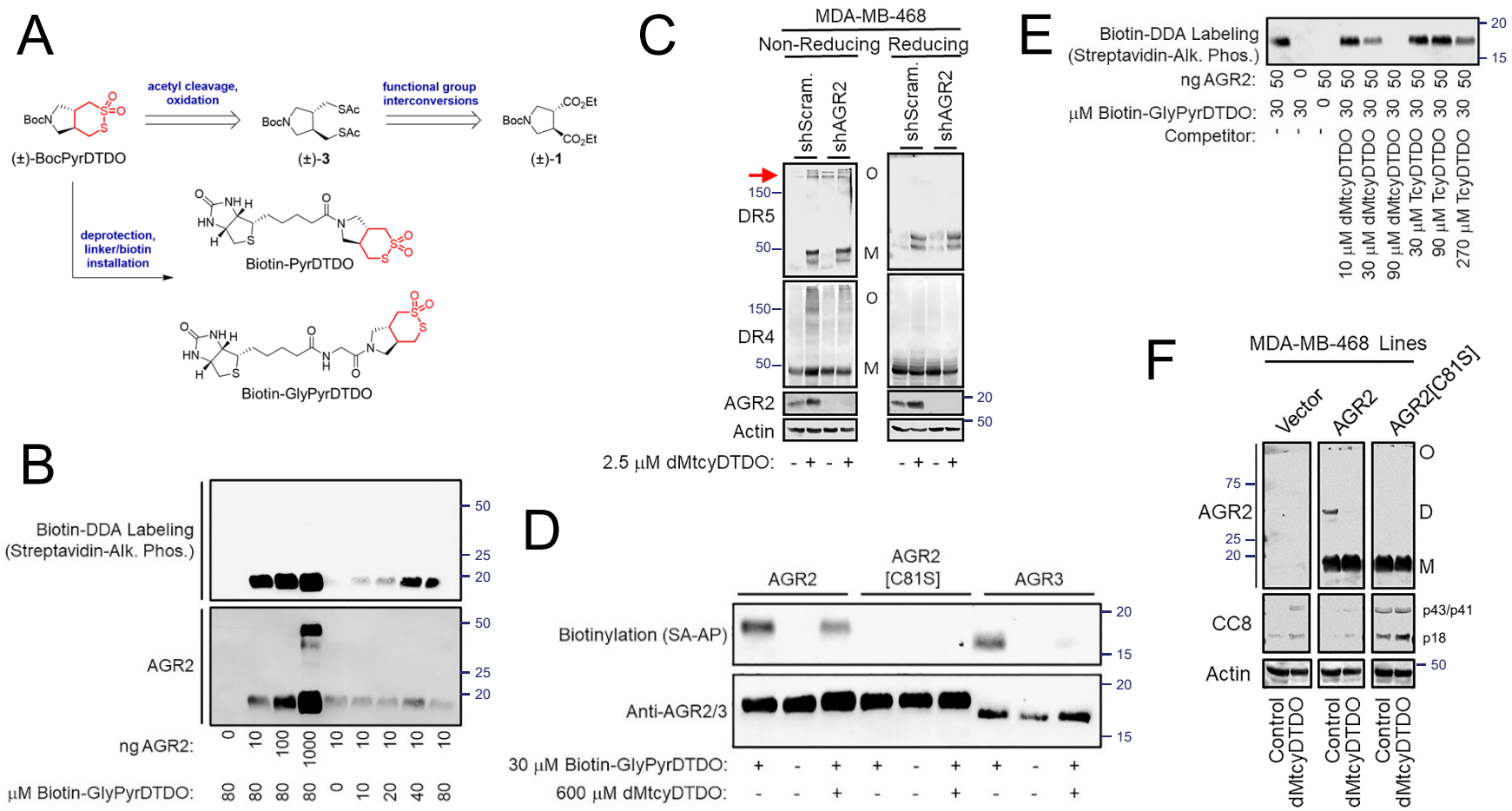

Fig. 2, Law et al.

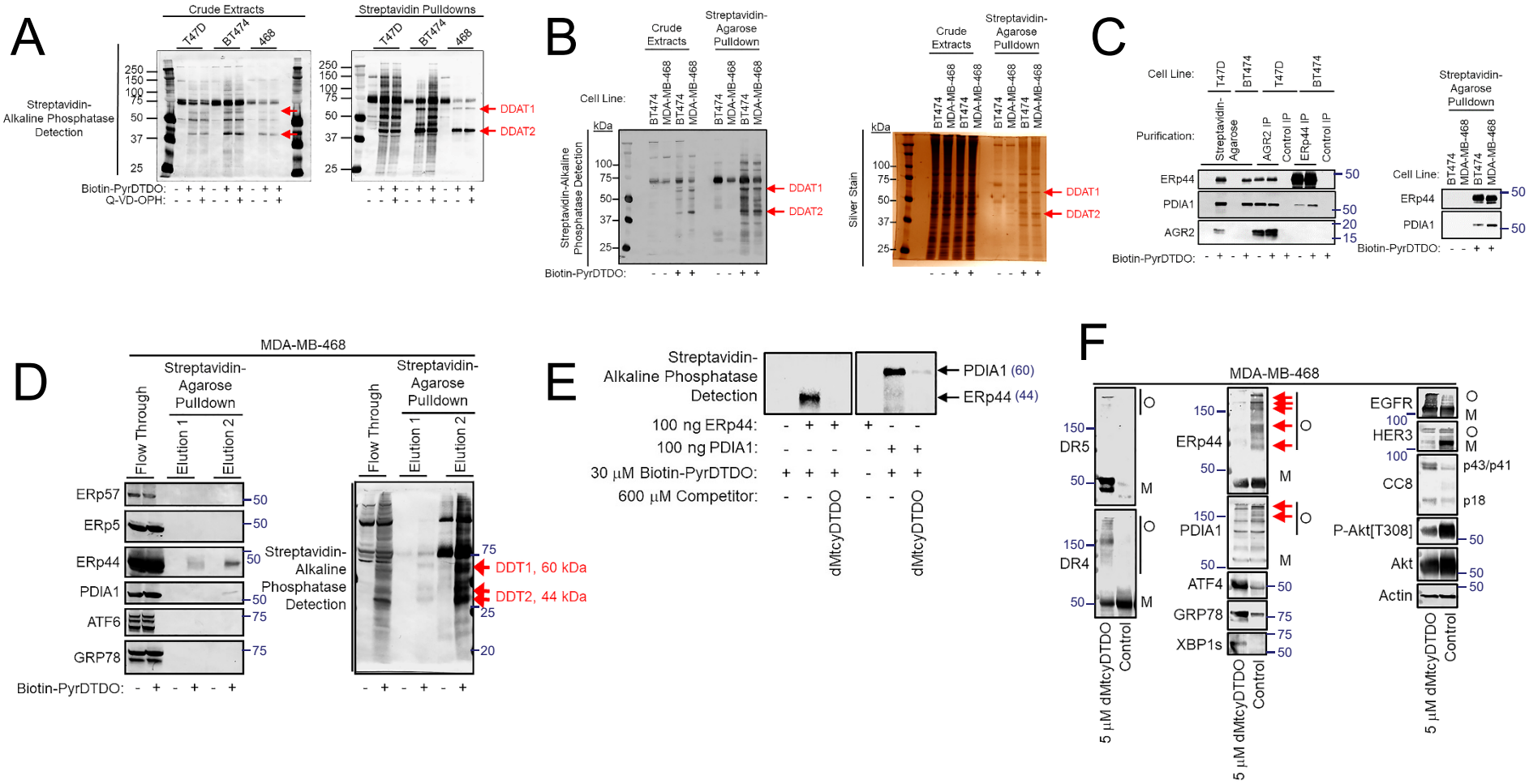

Fig. 3, Law et al.

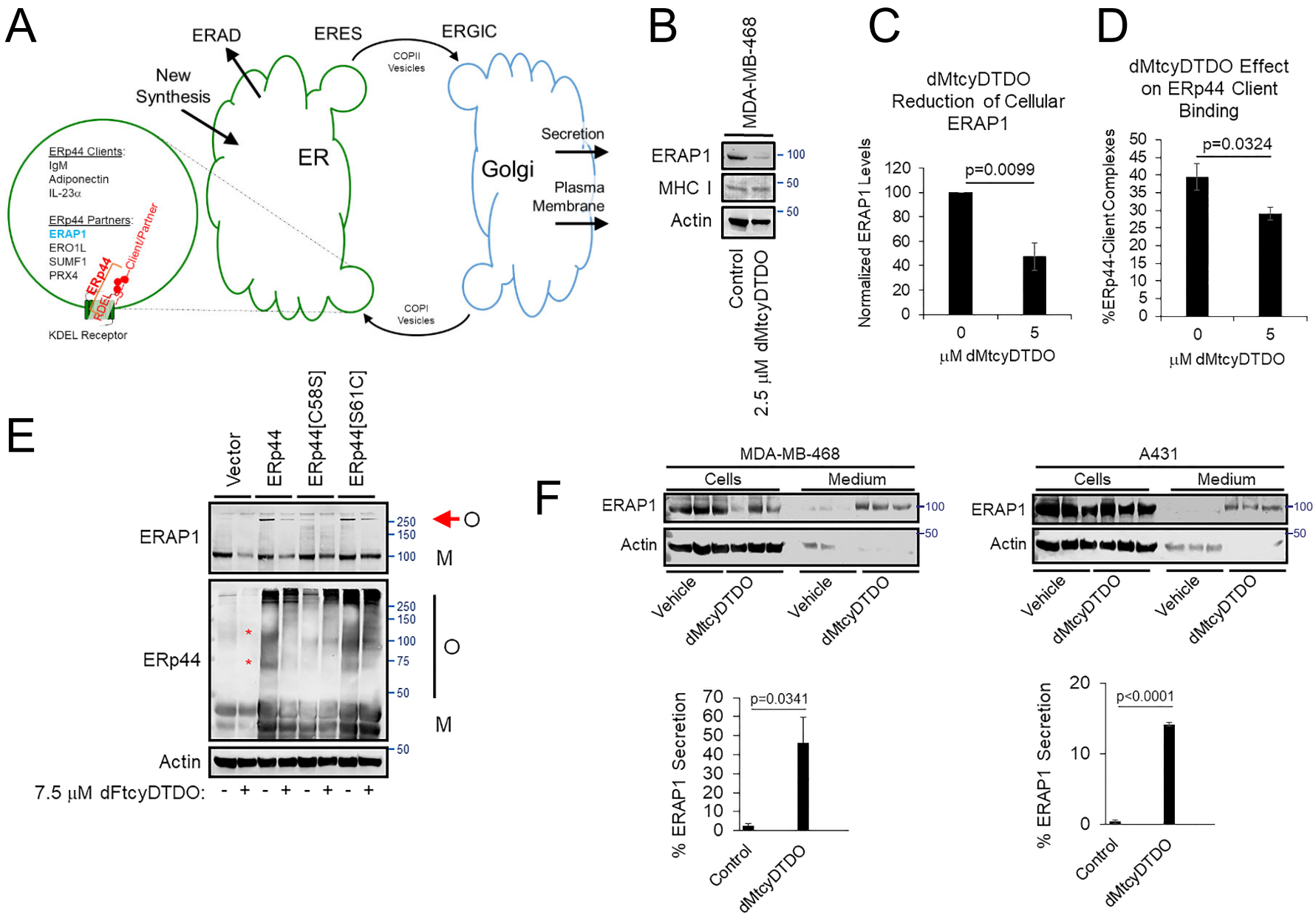

Fig. 4, Law et al.

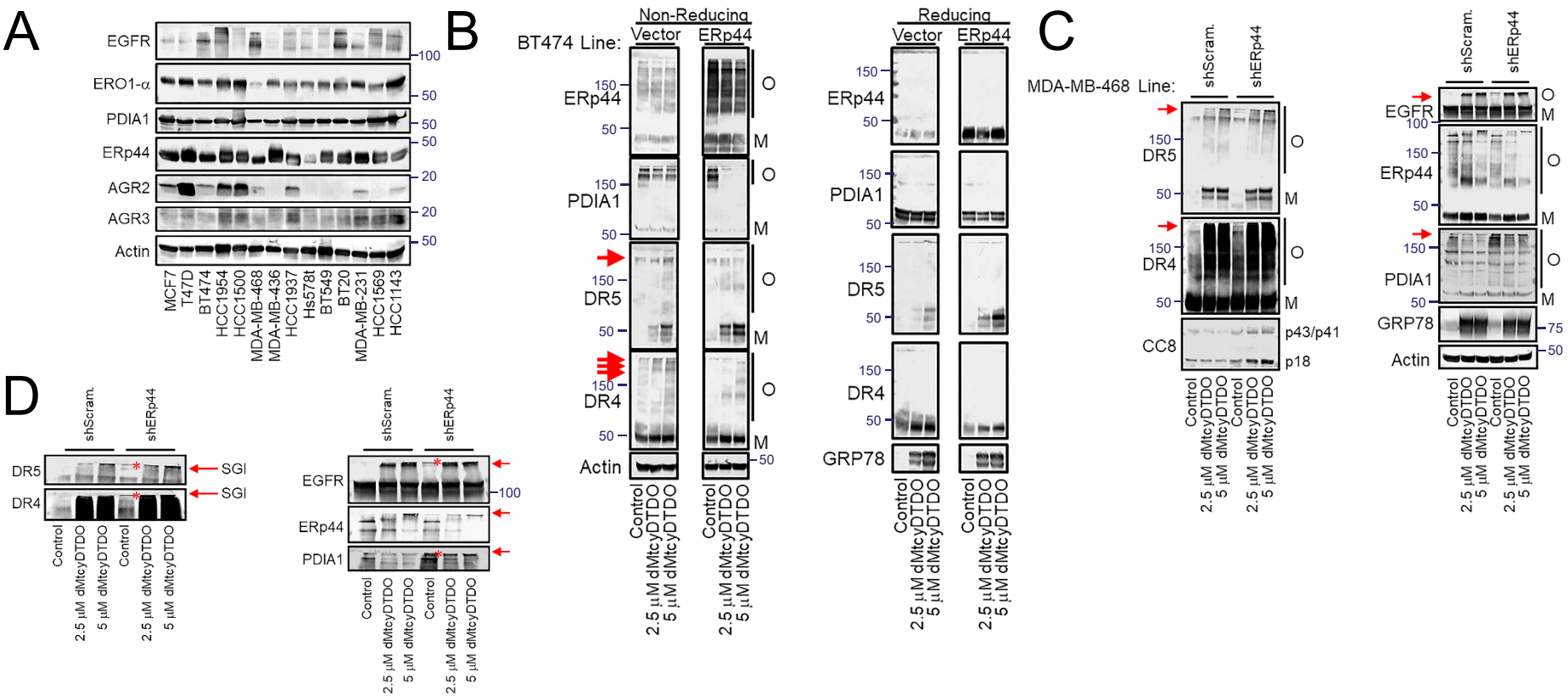

Fig. 5, Law et al.

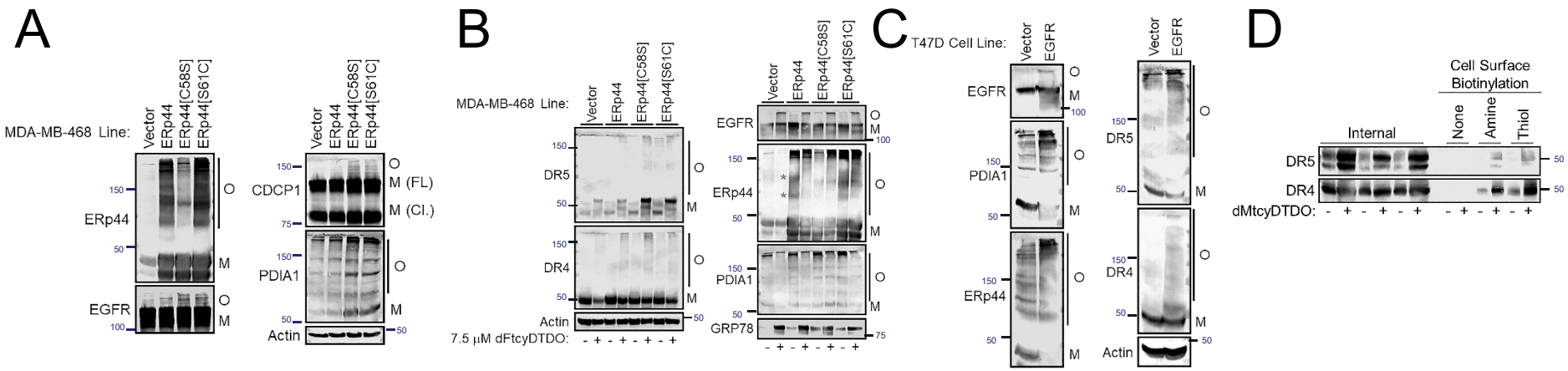

Fig. 6, Law et al.

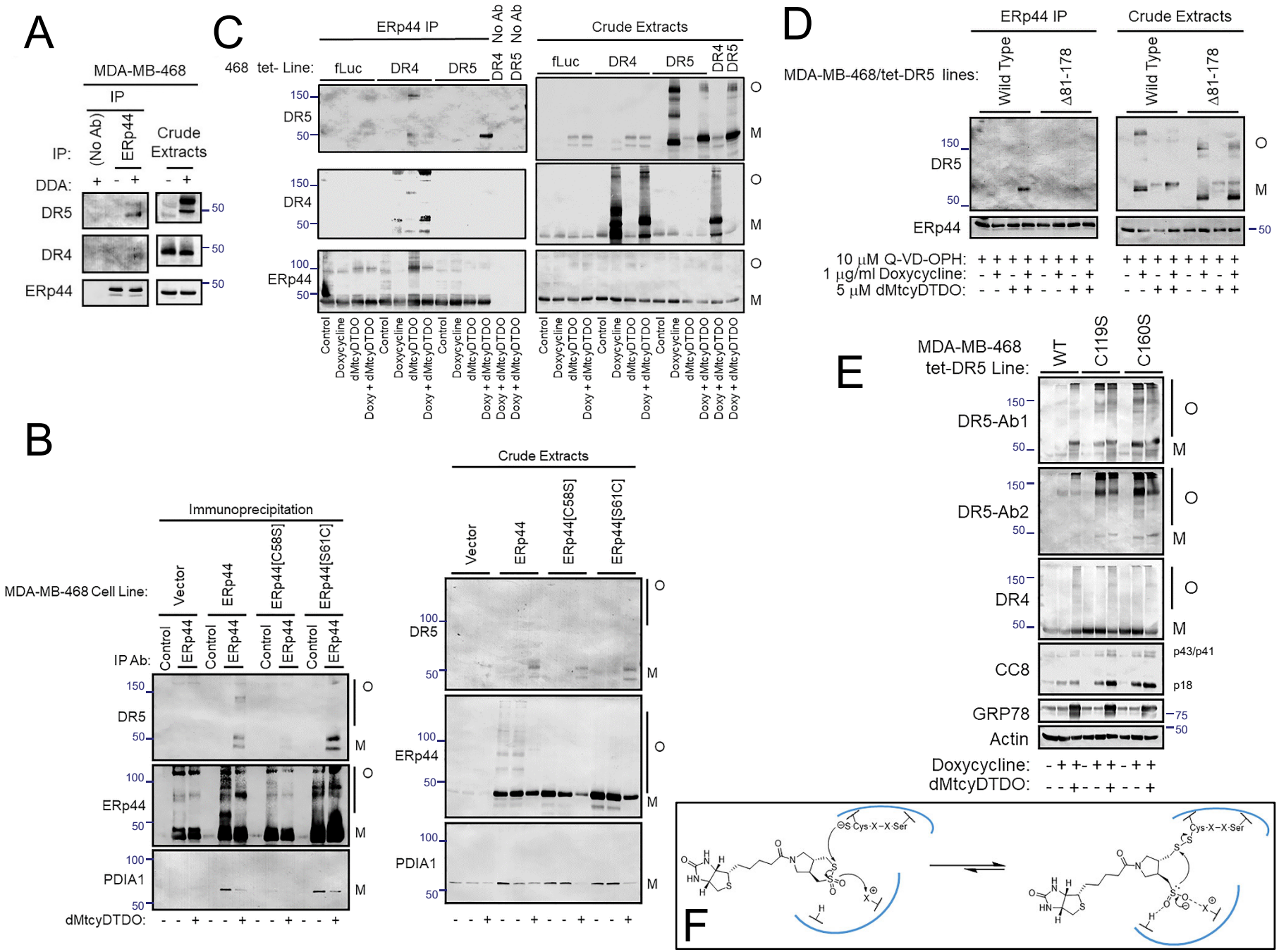

Fig. 7, Law et al.